Excerpt from the Proceedings of the 2011 COMSOL Conference in Boston

Study on the Holding Characterestics of a Magnetic Gripper

Rhythm S. Wadhwa[*1], Terje Lien[2] and Gareth Monkman[2]
[1]NTNU, [2]NTNU, [3]Hochschule Regensburg
*Corresponding author: NTNU Valgrinda, Inst. for produksjons- og kvalitetstek., Trondheim, 7491, Norway, rhythmsuren@ieee.org

Abstract: This paper explores the optimal design of an electromagnet tip, to enable robust pick and place activity by an industrial robot. Knowledge of the magnetic field gradients and gripper holding forces is necessary prerequisite to determine if a part might during handling operation.(1) A gradient depends strongly on the design of electromagnet tip. First, a magnetic circuit model was developed which when compared to the experimental data was found to be limited in its ability to accurately predict the holding force. A three dimensional finite element model was then developed using COMSOL Multiphysics to overcome these limitations. Predictions with this model were found to be in better agreement with the experiments, providing errors within 25 percent in most cases.

Keywords: Magnetic Gripping, Robot Handling.

1. Introduction

Robot grippers are used to position and retain parts in an automated assembly operation. In conventional foundry assembly, such grippers are dedicated to large volume handling of standard parts. The cost of the grippers may be as high as 20% of a robot's cost, depending on the application and part complexity (6). Electromagnet grippers have several advantages for handling ferrous parts over conventional impactive, ingressive or contiguitive grippers. (5)(1) These grippers offer simple compact construction with no moving parts, uncomplicated energy supply, flexibility in holding complex parts and reduced number of set-ups (5). However, their use is limited to ferrous materials (Iron, Nickel, Cobalt), electromagnet size is directly dependant on required prehension force; residual magnetism in the part when handled when using DC supplies requires the additional of a demagnetizing operation to the manufacturing process. While the choice of material limits application, and demagnetizing is a requirement, the holding force is an important unknown.

Figure 1.0 illustrates the working principle of an electromagnetic gripper.

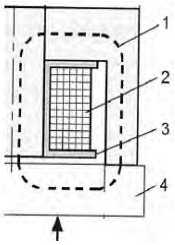

Figure 1. Principle of Electromagnetic Gripper

When placed in contact with an electromagnet, the part provides a flow path for the magnetic flux that completes the magnetic circuit. The force of attraction produced by this circuit holds the part against the electromagnet. During the robot motion, the part tends to slip against the electromagnet surface if the tangential holding force in that direction exceeds the limiting force of static friction for the magnet-part contact. This component of the holding force is in turn dependent on the holding force normal to the electromagnet surface via the coefficient of static friction for the magnet-part material pair (5).

In this paper we present the design of an electromagnet that produces the necessary magnetic field properties in an active volume of $3x3x3\,cm^3$, which is of interest to the participating foundry. Many forms of tips were implemented and compared in order to finally obtain the design to assure the availability of a magnetic flux density of 210 mT and a field gradient 12 T/m in the targeted volume.

2. Experimental Setup

The electromagnet robot automation cell was installed between the Fettling and the Assembly area in the Foundry. [1]

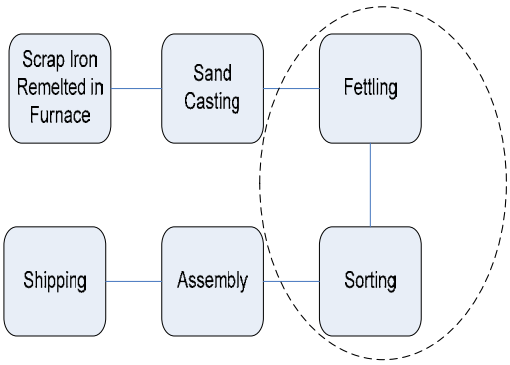

Figure 2. Foundry Process Map

The six axis ABB ERB 6400 robot used is shown in Figure 3.0. An overhead camera was used for identifying the orientation of the part lying on the conveyor belt, which was internally tracked by the robot. The image captured by the camera was processed and transferred via closed network Ethernet connection to the Robot. The robot gripper then moved the electromagnets accordingly to pick the part.

Figure 3. Robot Assembly Cell set up

Figure 4. Gripper head shapes tested

The parts were made of cast iron with the following nominal chemical composition: 3.2 percent Carbon, 2.65 percent Silicon, 0.45 percent Phosphorus, 0.45 percent Manganese, 0.05 percent Sulphur, 0.09 percent Chromium and 0.002 percent Lead.

While the layout provided in this paper are based on real assembly shop data in a company, the actual production volumes and assembly station rates are not revealed due to proprietary nature of the information.

3. Magentic Circuit Model

The magnetic circuit approach is an analytical method, analogous to electric circuit analysis, for modeling electromagnetic devices (4). The driving force in a magnetic circuit is the magnetomotive force (MMF) $\Im$ which produces a magnetic flux against a coil reluctance $\Re$. The reluctance is defined as:

$$\Re = \frac{l}{\mu A} \qquad [1]$$

Where l is the length of the magnetic flux path, A is the cross section area perpendicular to the flux, and μ is the permeability of the material.

For a given MMF and $\Re$, the flux ϕ in the circuit can be found from Kirchoff's law for magnetic circuits. The holding force can be computer using the following simple relation (5):

$$F = \frac{B^2 A}{2\mu_0} \qquad [2]$$

Where B represents the magnetic flux density in the airgap separating the components, A is the cross section area of the airgap and μ_0 is the permeability of air.The flux depends on the overall reluctance of the system. The reluctance is low when there is perfect contact between the part and electromagnet. However, part form errors, e.g., roughness (Figure 5.0), and deviation from flatness give rise to air gaps between the part and gripper.

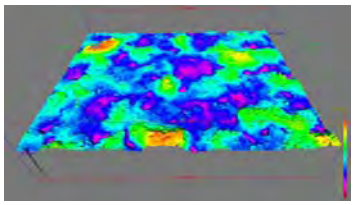

Figure 5. Surface roughness of the casted part

Since actual size and distribution of the airgaps in the gripper-part interface are difficult to determine for a gripper directly in contact with the part surface; it is proposed to model a small uniform air gap that can be reproduced in an experiment. It can be assumed here that the reluctance of this air gap is equivalent to the reluctance of the actual contact.

The reluctances proposed in this model include those of the electromagnet, air gaps, part, and the surrounding air medium. The procedure for modeling the reluctances is described next.

Electromagnet Reluctance $\Re_{Electromganet}$**.** Figure 1.0 shows the approximate magnet geometry used to calculate the average cross sectional areas and to simplify the shape path of the flux lines. Note, only a quarter of the cylindrical electromagnet is considered.

Part Reluctance $\Re_{Part}$**.** The ring-shaped part [ASTM Standard 773] has a nonuniform cross section perpendicular to the magnetic flux. The part reluctance is calculated using the following equation (3):

$$\Re_{Part} = \oint \frac{dl}{\mu(l).A(l)} \qquad [3]$$

To evaluate this line integral, a numerical integration scheme can be used. The mean path is such that it is normal to the radial line representing the cross sectional area. The variation in part permeability along the flux path is explicitly accounted for in the calculation of the circuit reluctance.

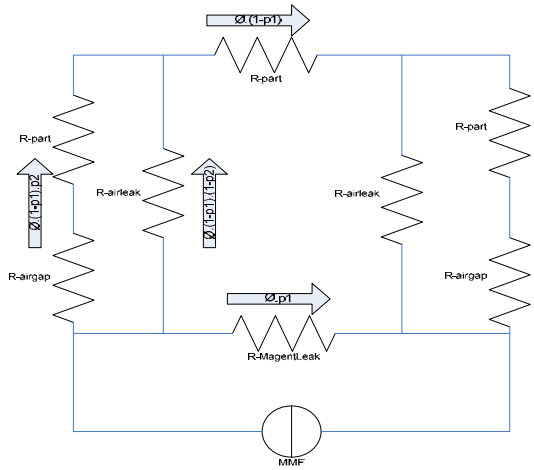

Figure 6. Equivalent Magnetic Circuit of the Magnet-Part System

Airgap Reluctance $\Re^{Airgap}$**.** The airgap term applies to the flux lines crossing the magnet-part interface. In reality, the airgap length varies at each point in the interface because of surface roughness and form errors. In this model, an equivalent uniform airgap length is used. The cross-sectional area of the air gap is equal to the magnet-part contact area.

Of the simplifications made above, the use of a mean magnetic flux path is most significant since it implies that the magnetic circuit model cannot predict the distribution of flux in the magnet-part system. However, it can still be used to estimate the total normal holding force and to gain an insight into the effects of magnet and part variables. The magnetic circuit model shown in Figure 6 took approximately 15 seconds to solve on a 2.6 GHz computer. Experimental validation of the magnetic circuit model showed that it had a limited range of applicability due to its inability to model nonuniform magnetic flux distribution and leakage. It is possible to overcome the drawbacks of the magnetic circuit model and increase its prediction accuracy through finite element method.

4. Use of COMSOL Multiphysics

COMSOL Multiphysics has been used to study and test multiple possible magnet forms to optimize the magnetic force. To compute and plot the magnetic flux density around the system tip, the model of the electromagnet was

implemented in 2D, as well as in 3D.The area of interest experiences a magnetic force according to the formula $F_{mag} = \mu.\nabla B$, where μ is the magnetic moment of a given particle and ∇B is the gradient of the magnetic field.

The involved Maxwell equations are: $\nabla xH = J$ and $\nabla B = 0$, with constitutive relation $B = \mu_0 \mu_r H$. The magnetic vector potential A produces the governing equation $\nabla x(\mu^{-1}\nabla xA - M) = J$ of the Magnetostatics module in COMSOL version 4.2.

Results

Concept of the Magnet

The electromagnet consists of an iron core, a yoke and a coil of copper. The iron yoke enforces the magnetic flux density. The figure 7 and 8 below show the drafts for the core and the yoke.

Figure 7. Design of the iron core and the yoke

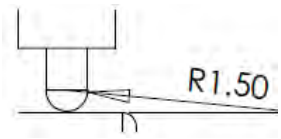

Figure 8. Dimensioning of the magnetic tip

The mean B-H curve for the magnet material was obtained from the supplier and that of the part was obtained experimentally. [ASTM Standard 773]

Calculation of the coil

The external current density was determined to 1.80e6 A/m^2. Table 3 (Appendix) indicates other parameters. The desired magnetic field results from the 7^o taper in the form of the magnet. With the distance from the tip the flux density falls rapidly. The field gradient ranges ffrom 28 T/m for a distance of 1mm to 11 T/m at a distance of 2mm from the magnet surface.

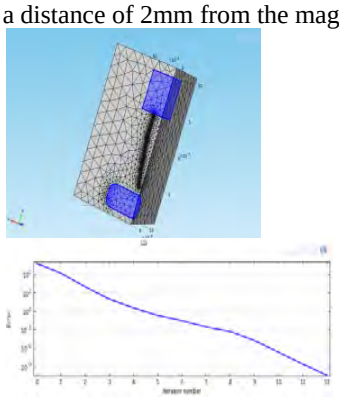

Figure 9. Finite Element Mesh and the convergence plot

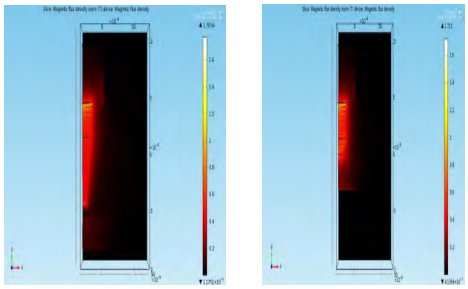

Figure 10. Magnetic field gradient: conical tip with with 1mm air gap and spherical tip with 0.1mm air gap

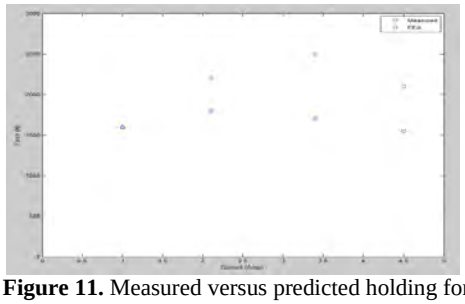

Figure 11. Measured versus predicted holding force

5. Conclusions

This paper presents two approaches for modeling magnetic flux density for electromagnets. The two methods consisted of the magnetic circuit approach and the finite element method using COMSOL Multiphysics.

Experimental validation of the magnetic circuit model showed that it had a limited range of applicability due to its inability to model nonuniform magnetic flux distribution and leakage.

In contrast, the finite element model in COMSOL Multiphysics, although more complex, was able to represent the distributed magnetic field, and yielded better results. The normal force prediction errors were found to be within 25 percent in most cases.

6. References

1. R.S.Wadhwa, T.Lien and G.J.Monkman Robust Prehension for ferrous metalcasted product families, *Proceedings of MITIP*, 2011

2. Campbell, in *Castings*. Butterworth-Heinemann, 2003

3. S.R.Hoole *Computer Aided Analysis and Design of Electromagnetic Devices*, 1989

4. J.D.Law *Modeling of Field Regulated Reluctance Machines*, PhD Thesis, University of Wisconsin Madison, 1991

5. G.J.Monkman and S.H.Steinmann *Robot Grippers*, Wiley-VCH, 2007

6. D.T.Pham and E.Tacgin An expert system for selection of robot grippers. Expert Systems with Applications,1992, 5, 289-300

7. Appendix

Table 1: Magnetic Constants

Magnetic Constants	Value
Relative Permeability (μ_r)	4e3 (Iron)
External Current density ($J_o\varphi$)	1.79 A/m^2

Table 2: Magnetostatic Equations

Magnetostatic Equations	Value
Magnetic Insulation	$A_\varphi = 0$
Continuity	$nx(H_1 - H_2) = 0$
Relative Permeability	Isotropic in each subdomain

Table 3: Parameters of the Coil

Diameter of the Copper Wire	$d = 1.22mm$
Cross-section of the wire	$A_L = 1.13mm^2$
Average length of the winding	$l_m = 34.56cm$
Number of windings	$N = 3714$
Length of the coil	$l = 1283.56m$
Mass of the coil	$m = 12.95kg$
External current density	$J = 1.79e6A/m^2$
Output voltage	$U = 41.14V$
Output current	$I = 2.04A$